Electronic Supplementary Information

Efficient and Robust Lithium Metal Electrodes Enabled by Synergistic Surface Activation–Passivation of Copper Frameworks

Jonghyeok Yun,‡[a] Eun-Seo Won,‡[b] Hyun-Seop Shin,[c] Kyu-Nam Jung,[c] and Jong-Won Lee*[a]

[a] *Department of Materials Science and Engineering, Chosun University, 309 Pilmun-daero, Dong-gu, Gwangju 61452, Republic of Korea. E-mail: jongwon@chosun.ac.kr*

[b] *Department of Biochemical and Polymer Engineering, Chosun University, 309 Pilmun-daero, Dong-gu, Gwangju 61452, Republic of Korea*

[c] *Energy Efficiency Technologies and Materials Science Division, Korea Institute of Energy Research, 152 Gajeong-ro, Yuseong-gu, Daejeon 34129, Republic of Korea*

‡ These authors contributed equally to this work.

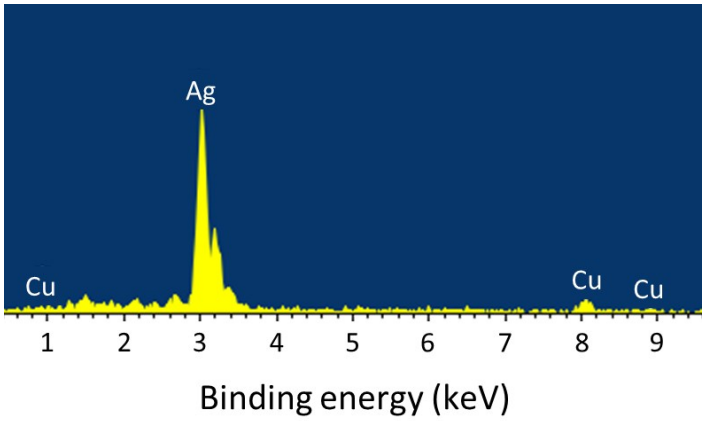

Fig. S1 EDS spectrum of 3D-Cu@Ag subjected to GD for t_{GD} = 10 s.

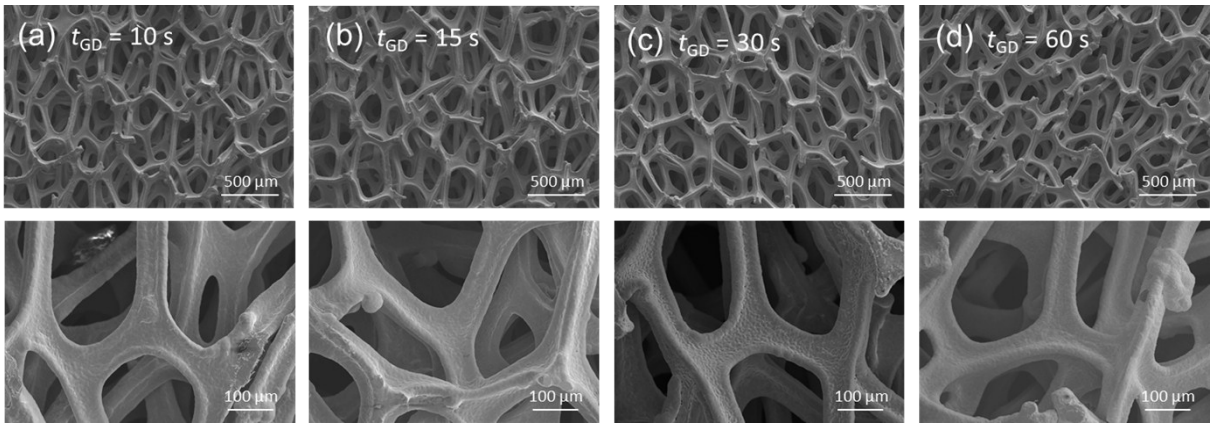

Fig. S2 Low-magnification SEM images of 3D-Cu@Ag frameworks for (a) t_{GD} = 10 s, (b) t_{GD} = 15 s, (c) t_{GD} = 30 s, and (d) t_{GD} = 60 s.

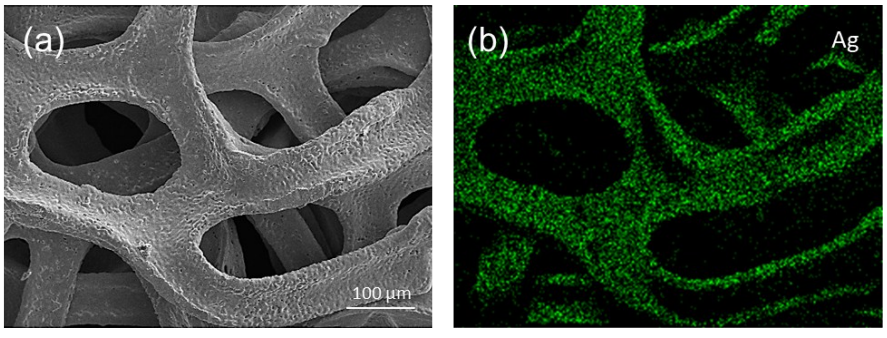

Fig. S3 (a) SEM image (top view) of 3D-Cu@Ag for t_{GD} = 10 s and (b) the corresponding EDS mapping result for Ag.

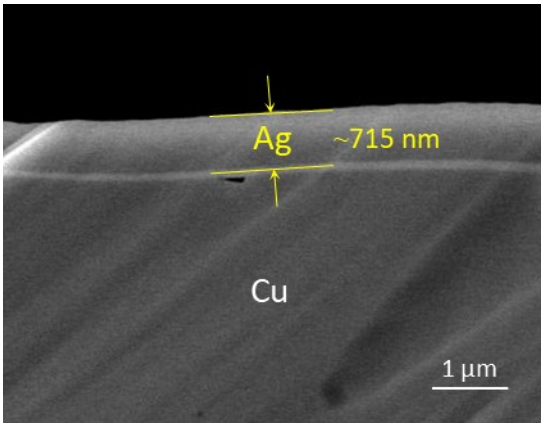

Fig. S4 Cross-sectional SEM image of 3D-Cu@Ag for t_{GD} = 15 s.

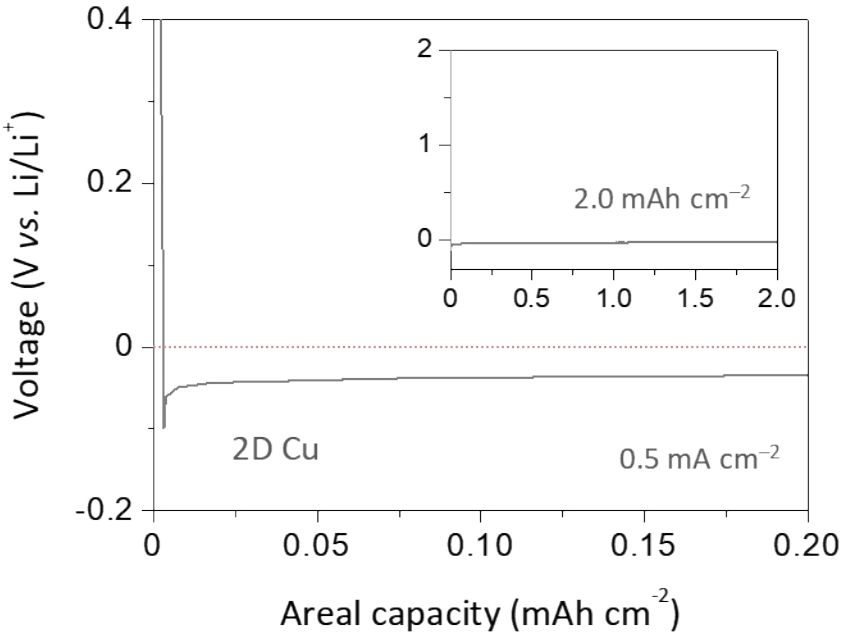

Fig. S5 Voltage profile of the 2D Cu foil measured during Li plating (2.0 mAh cm^{-2} at 0.5 mA cm^{-2}).

Fig. S6 Photographs of 2D Cu and Cu@Ag foils. The 2D Cu@Ag foil was prepared by the GD process for t_{GD} = 10 s.

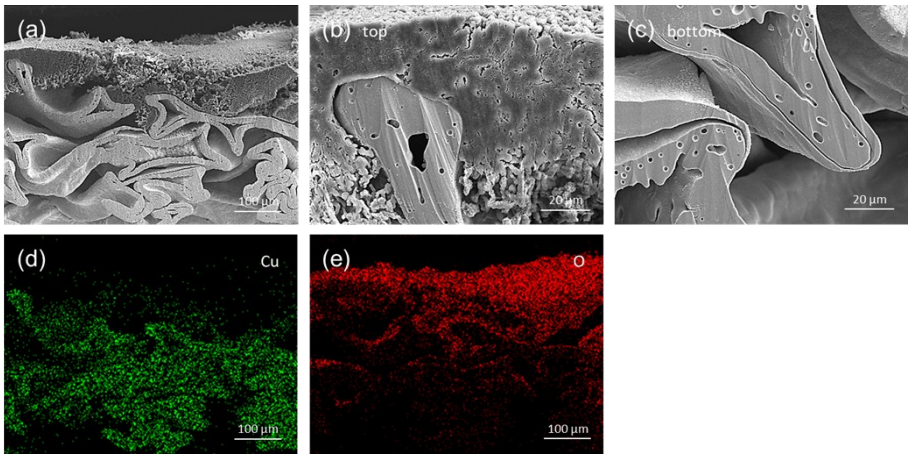

Fig. S7 (a–c) Cross-sectional SEM images of 3D-Cu taken after Li plating (2.0 mAh cm^{-2} at 0.5 mA cm^{-2}) and (d, e) the corresponding EDS mapping results for Cu and O. The electrode was exposed to ambient atmosphere prior to EDS analysis, and the oxygen signal was recorded to determine the spatial distribution of LiO_x.

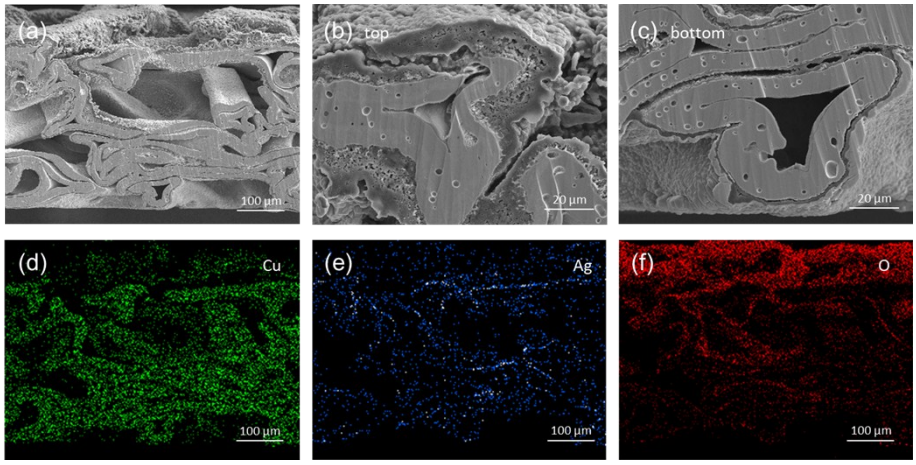

Fig. S8 (a–c) Cross-sectional SEM images of 3D-Cu@Ag taken after Li plating (2.0 mAh cm^{-2} at 0.5 mA cm^{-2}) and (d–f) the corresponding EDS mapping results for Cu, Ag, and O. The electrode was exposed to ambient atmosphere prior to EDS analysis, and the oxygen signal was recorded to determine the spatial distribution of LiO_x.

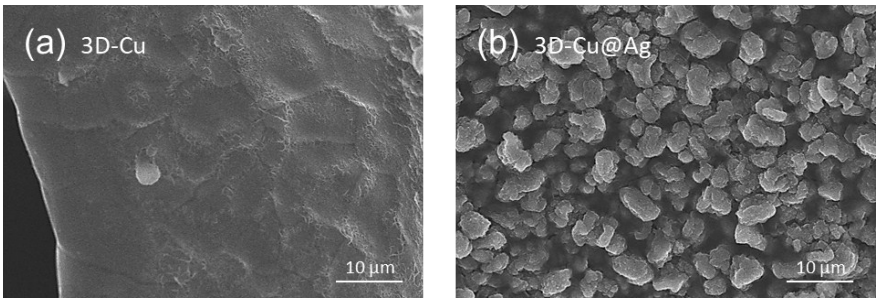

Fig. S9 SEM images of (a) 3D-Cu and (b) 3D-Cu@Ag taken from the surfaces without Li dendrites. Li plating was performed with 2.0 mAh cm^{-2} at 0.5 mA cm^{-2}.

Note 1. Equivalent circuit and modeling analysis of Li plating

Li plating in a 3D framework involves the two reactions: (1) Li plating on the top surface (on the separator side) (designated as '1' in Figure 5a) and and (2) Li plating inside the pore (designated as '2' in Figure 5a).

(1) Reaction 1: Li plating on the planar top surface involves interfacial charge-transfer and double-layer charging, and thus, it is simply described by an equivalent circuit (Z_s) consisting of $R_{ct,s}$ and $C_{d,s}$ connected in parallel.

(2) Reaction 2: Li plating in a pore involves Li^+ migration in the electrolyte-filled pore and interfacial charge-transfer, double-layer charging. This process can be described by a modified transmission line (Z_p) that has a network of distributed resistive and capacitive elements. As illustrated in Figure 5b, Z_p is composed of (i) series-connected $r_{i,p}$ elements related to Li^+ migration in the pore and (ii) parallel-connected $r_{ct,p}$ and $c_{d,p}$ associated with interfacial charge-transfer and double-layer charging.

Given that the two Li plating processes on the top surface (1) and in a pore (2) are indepedent of each other, Z_s and Z_p are connected in parallel. For simulations, Z_p was constructed with 20 distributed elements of $r_{i,p}$, $r_{ct,p}$, and $c_{d,p}$ (i.e., n = 20), and the following parameters and assumptions were used: electrode area = 2.05 cm^2; electrode thickness = 500 μm; cylindrical pore shape; pore diameter = 250 μm; distance between pores = 100 μm; electrolyte conductivity = 1.0×10^{-2} S cm^{-1}; double-layer capacitance = 1.0×10^{-5} F cm^2; exchange current density = 1.0×10^{-3} A cm^{-2}.[S1]

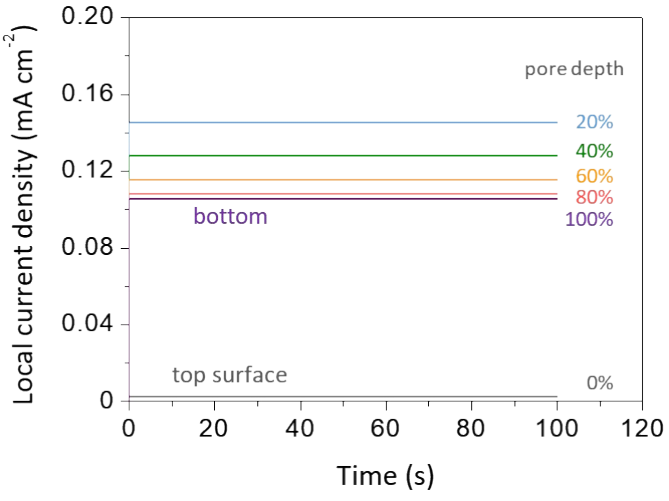

Fig. S10 Local current densities on different locations of the 3D framework calculated using $R_{ct,s}$ = 2,570 Ω cm^2 and exchange current density = 0.67×10^{-3} A cm^{-2}. The total current density was 0.5 mA cm^{-2}.

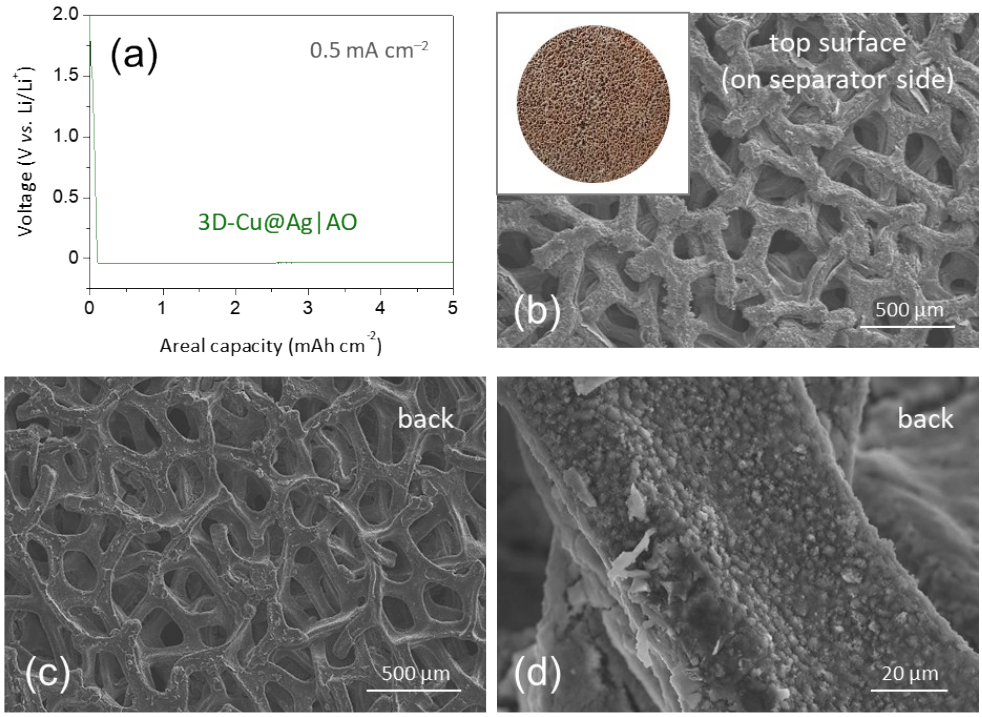

Fig. S11 (a) Voltage profile of 3D-Cu@Ag|AO measured during Li plating (5.0 mAh cm^{-2} at 0.5 mA cm^{-2}) and (b–d) SEM images taken after Li plating: (b) top surface (facing the separator) and (c, d) back side. The photograph of the electrode was also included in the inset of (b).

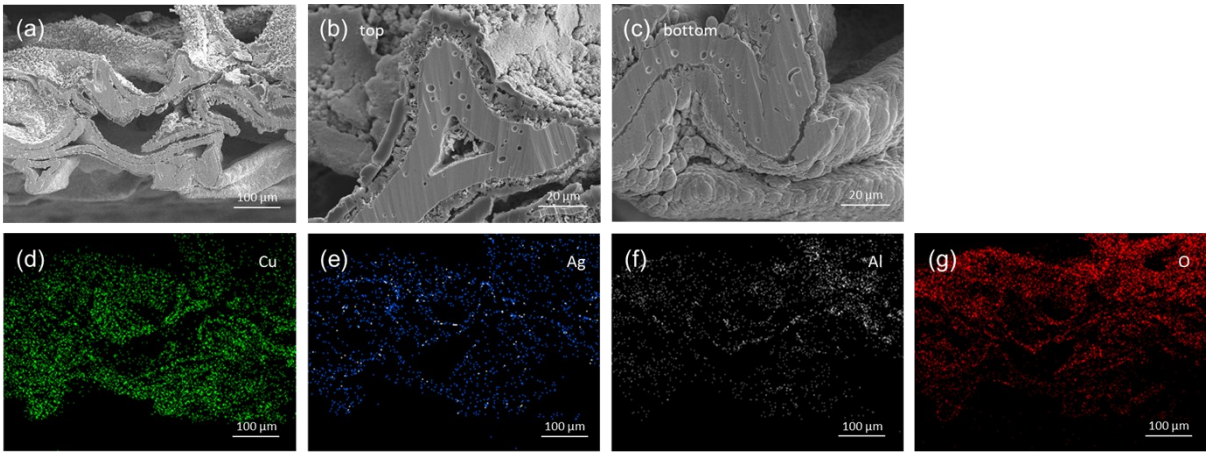

Fig. S12 (a–c) Cross-sectional SEM images of 3D-Cu@Ag|AO taken after Li plating (2.0 mAh cm^{-2} at 0.5 mA cm^{-2}) and (d–g) the corresponding EDS mapping results for Cu, Ag, Al, and O. The electrode was exposed to ambient atmosphere prior to EDS analysis, and the oxygen signal was recorded to determine the spatial distribution of LiO_x. Note that the O signal originated from both LiO_x and Al_2O_3.

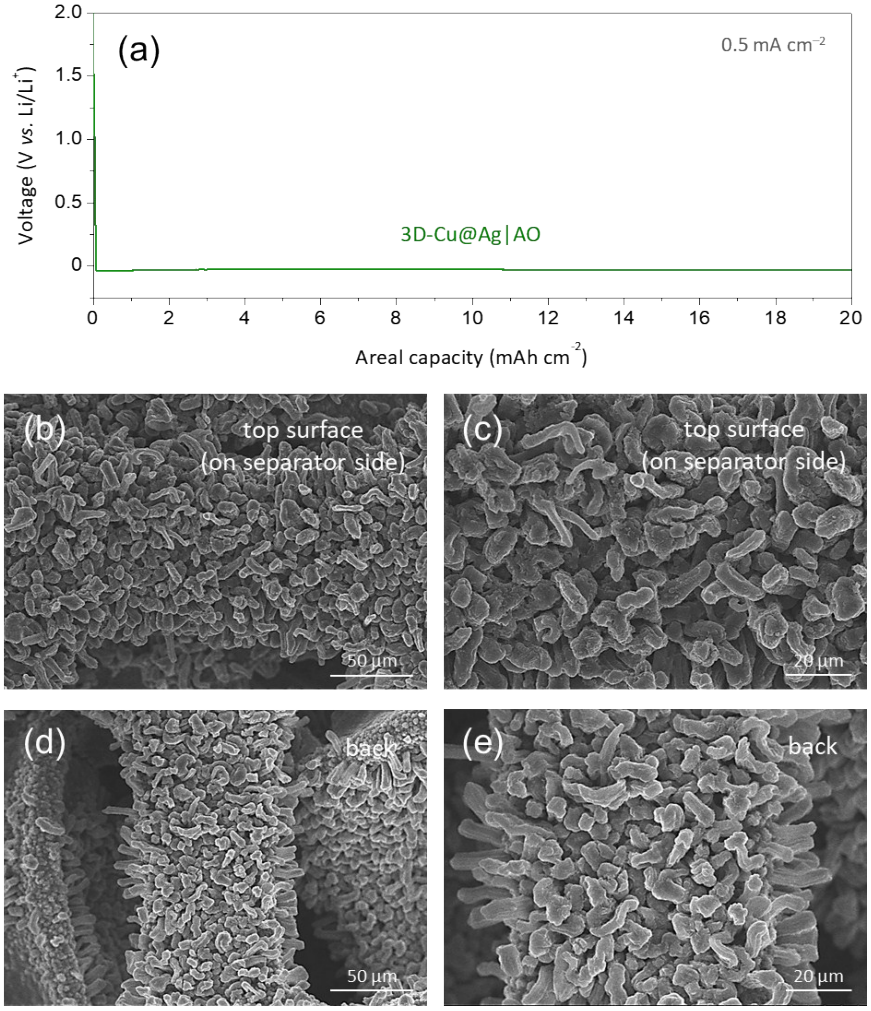

Fig. S13 (a) Voltage profile of 3D-Cu@Ag|AO measured during Li plating (20 mAh cm^{-2} at 0.5 mA cm^{-2}) and (b–e) SEM images taken after Li plating: (b, c) top surface (facing the separator) and (d, e) back side. Note that Li deposits were observed on both top and back sides.

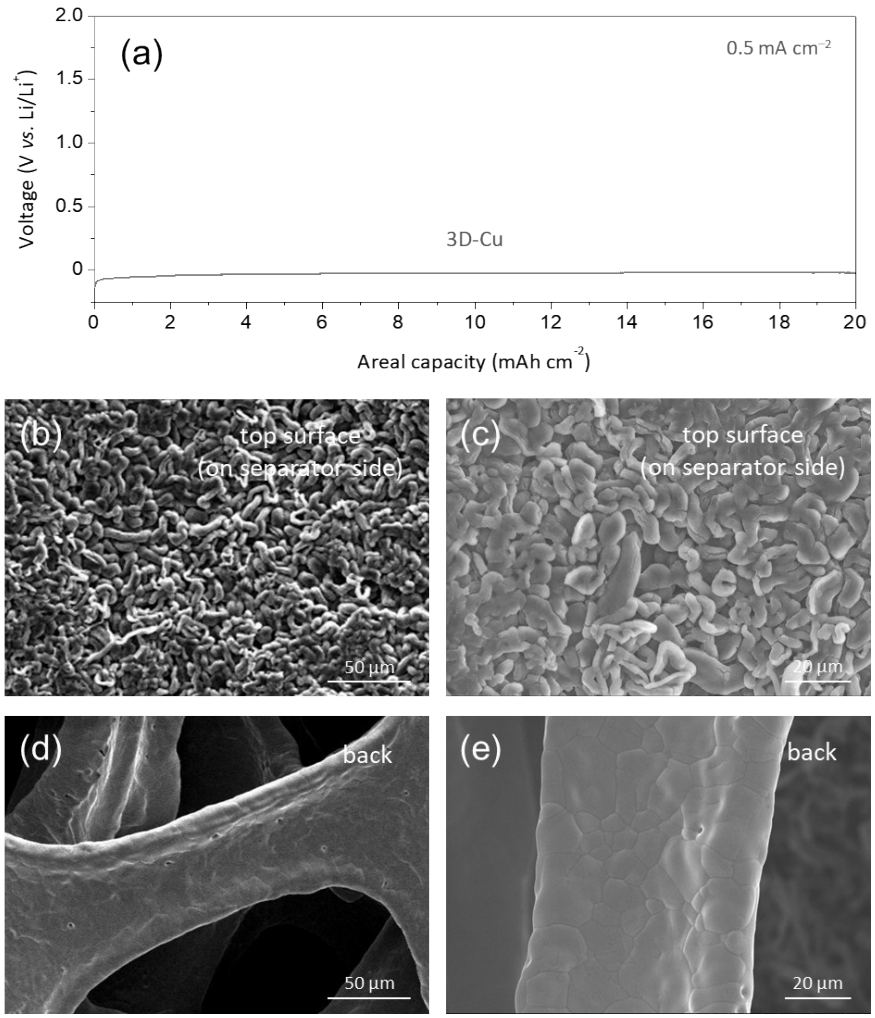

Fig. S14 (a) Voltage profile of 3D-Cu measured during Li plating (20 mAh cm^{-2} at 0.5 mA cm^{-2}) and (b–e) SEM images taken after Li plating: (b, c) top surface (facing the separator) and (d, e) back side. Note that Li deposits were only observed on the top surface.

Note 2. Estimation of Coulombic efficiencies (CEs)

The CE value was determined using the following procedure proposed by Adams et al.[S2]:

(1) Pre-conditioning by Li plating to 2.0 mAh cm^{-2} at 1.0 mA cm^{-2} and subsequent Li stripping at 1.0 mA cm^{-2} to 1.5 V vs. Li/Li$^+$;

(2) Plating of Li reservoir (Q_T = 2.0 mAh cm^{-2}) at 1.0 mA cm^{-2};

(3) 10 cycles (n = 10) of Li plating–stripping (Q_C = 1.0 mAh cm^{-2}) at 0.5, 1.0 or 2.0 mA cm^{-2};

(4) Full Li stripping at 1.0 mA cm^{-2} to 1.5 V vs. Li/Li$^+$ (Q_S).

The average CE value was calculated by

$$\mathrm{CE} = \frac{nQ_C + Q_S}{nQ_C + nQ_T} \tag{S1}$$

Table S1 Coulobmic efficiencies (CEs) of 3D frameworks measured at various current densities.

Current density (mA cm^{-2})	CE (%)		
	3D-Cu	3D-Cu@Ag	3D-Cu@Ag|AO
0.5	93.8	96.3	98.5
1.0	92.9	95.6	98.2
2.0	92.1	94.5	96.9

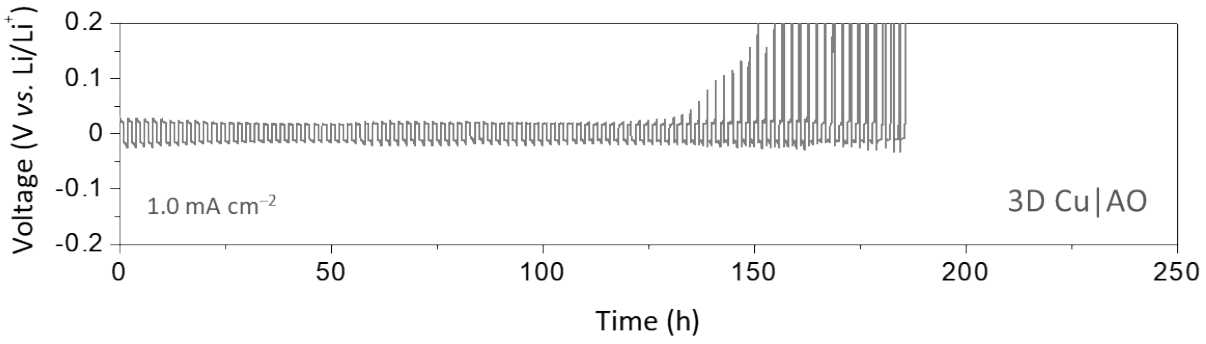

Fig. S15 Cycling performance for 3D-Cu|AO at 1.0 mA cm^{-2}.

Table S2 Comparisons of technical approaches and electrochemical performance of various various Cu-based 3D frameworks for Li electrodes.

Electrode	Technical approach	Current density* (mA cm^{-2})	Capacity* (mAh cm^{-2})	CE (%)	Reference
3D Cu	H_2 bubble dynamic template	0.5	1	~97	S1
3D Cu	Electrochemical dealloying of Cu–Zn	1	1	97.9	S2
VA-CuO-Cu	Vertically aligned CuO nanosheets	0.5	1	94	S3
Cu_2S NWs/Cu	In situ growth of Cu_2S nanowires on Cu foam	1	1	95.5	S4
3D Cu submicron skeleton	$Cu(OH)_2$ deposition, dehydration, reduction	0.5	1	97	S5
	with 0.005M Li_2S_6 additive	0.5	1	98.5	S6
Cu NW	Solvent evaporation assisted assembly *(with 0.005M Li_2S_8 additive)*	1	1	98.6	S7
3D Cu mesh	Controlled mesh size	0.5	1	93.8	S8
3D Cu	Vacuum distillation of Cu–Zn	0.52	0.26	~90	S9
Cu-CuO-Ni	Cu-CuO nanowire arrays on Ni foam	1	1	~95	S10
3D Cu film	Liquid Ga-induced alloying–dealloying	0.5	1	98.2	S11
		1	1	~97	S12
3D-Cu@Ag|AO	Ag nanolayer $Al2O_3$ passivating layer	1	1	98.2	This work

* Test conditions for CE evaluations

References

S1. P. Arora, M. Doyle and R. E. White, *J. Electrochem. Soc.*, 1999, **146**, 3543.
S2. B. D. Adams, J. Zheng, X. Ren, W. Xu and J.-G. Zhang, *Adv. Energy Mater.*, 2018, **8**, 1702097.
S3. H. Qiu, T. Tang, M. Asif, X. Huang and Y. Hou, *Adv. Funct. Mater.*, 2019, **29**, 1808468.
S4. H. Zhao, D. Lei, Y.-B. He, Y. Yuan, Q. Yun, B. Ni, W. Lv, B. Li, Q.-H. Yang, F. Kang and J. Lu, *Adv. Energy Mater.*, 2018, **8**, 1800266.
S5. C. Zhang, W. Lv, G. Zhou, Z. Huang, Y. Zhang, R. Lyu, H. Wu, Q. Yun, F. Kang and Q.-H. Yang, *Adv. Energy Mater.*, 2018, **8**, 1703404.
S6. Z. Huang, C. Zhang, W. Lv, G. Zhou, Y. Zhang, Y. Deng, H. Wu, F. Kang and Q.-H. Yang, *J. Mater. Chem. A*, 2019, **7**, 727.
S7. C.-P. Yang, Y.-X. Yin, S.-F. Zhang, N.-W. Li and Y.-G. Guo, *Nat. Commun.*, 2015, **6**, 8058.
S8. L.-L. Lu, J. Ge, J.-N. Yang, S.-M. Chen, H.-B. Yao, F. Zhou and S.-H. Yu, *Nano Lett.*, 2016, **16**, 4431.
S9. Q. Li, S. Zhu and Y. Lu, *Adv. Funct. Mater.*, 2017, **27**, 1606422.
S10. Y. An, H. Fei, G. Zeng, X. Xu, L. Ci, B. Xi, S. Xiong, J. Feng and Y. Qian, *Nano Energy*, 2018, **47**, 503.
S11. S. Wu, Z. Zhang, M. Lan, S. Yang, J. Cheng, J. Cai, J. Shen, Y. Zhu, K. Zhang and W. Zhang, *Adv. Mater.*, 2018, **30**, 1705830.
S12. Y. Shi, Z. Wang, H. Gao, J. Niu, W. Ma, J. Qin, Z. Peng and Z. Zhang, *J. Mater. Chem. A*, 2019, **7**, 1092.